



Changes of actual evapotranspiration and its components in the Yangtze River valley during 1980–2014 from satellite assimilation product

Jiao Lu¹ · Guojie Wang¹ · Tiantian Gong¹ · Daniel Fiifi T. Hagan¹ · Yanjun Wang¹ · Tong Jiang² · Buda Su²

Received: 12 December 2018 / Accepted: 27 May 2019 / Published online: 11 June 2019
© Springer-Verlag GmbH Austria, part of Springer Nature 2019

Abstract

Evapotranspiration (ET) is an important process of water and energy exchanges between land and atmosphere. In this study, a processed-based GLEAM (global land-surface evaporation: the Amsterdam methodology) satellite assimilation product has been validated in the Yangtze River valley on the observations of flux and the water balance method. The changes of total ET and its components, well as the associated dynamics, have been analyzed for the period of 1980–2014. The total ET shows significant increasing trends especially in the middle and lower reaches of the Yangtze River valley, which is mostly due to the increase of transpiration. The spatial and temporal dynamics of total ET are analyzed with respect to temperature, precipitation, and solar radiation. The spatial pattern of total ET in the Yangtze River valley is found to be jointly determined by temperature and precipitation. As for the temporal dynamics, precipitation plays the dominant role in total ET in the source regions of the valley. While in the most regions, solar radiation is suggested to be a main controller, in the positive manner, of total ET. This may provide an in-depth understanding of ET changes in the warming climate, and form a basis for water resource management in the Yangtze River valley.

1 Introduction

Terrestrial evapotranspiration (ET) is one of the core processes of the climate system which links the water, energy, and carbon cycles (Jung et al. 2010). It plays the key role in connecting water resources, agricultural management, carbon and climate feedbacks, and ecosystem functioning (Fisher et al. 2017). The changes of ET have become an effective tool for understanding the climate change impact on water cycle (Wang and Dickinson 2012), and many studies have indicated that the climate is also sensitive to the changes of land ET (Taylor et al. 2012). The global land ET provides about 60% of the moisture sources for precipitation (Oki and Kanae 2006), and a reduction of land ET leads to more energy being converted to sensible heat, so that the near-surface temperature rises.

Meanwhile, facing the water scarcity in the changing climate, we must make a rational use of regional water resources. This requires us to know more about the water consumption of the land surface under different land use conditions, where ET plays an essential role. However, actual ET is still the biggest unknown item in the global hydrological cycle at present. Actual ET has been upscaled from eddy covariance flux tower sites to the regional scale with machine learning algorithms (Xu et al. 2018). Basic theories, observational methods, various surface energy balance algorithms, and uncertainties and limitations related to those estimation methods for estimations of ET with remotely sensed surface temperatures have been surveyed (Liou and Kar 2014). Investigating the changes and the associated dynamics of land ET can help to reduce the uncertainties in our understanding of climate change impact on terrestrial water cycle and is also of great importance for us to understand the availability of water resources.

There are several comprehensive studies on the changes of global land ET in response to the warming climate. Global land ET showed different trends in different study periods. Wang et al. (2010a, b) found that the global land ET from 1982 to 2002 increased at a rate of 15 mm/year, based on observational records of 1120 globally distributed stations. Jung et al. (2010) studied global land ET from 1982 to 2008 using a combined database of FLUXNET, remote sensing,

✉ Guojie Wang
gwang@nuist.edu.cn

¹ Collaborative Innovation Center on Forecast and Evaluation of Meteorological Disasters, School of Geographical Sciences, Nanjing University of Information Science & Technology, Nanjing 210044, China

² National Climate Center, China Meteorological Administration, Beijing 100081, China

and meteorological observations; the global land ET was found to increase at a rate of 7.1 ± 1.0 mm per decade from 1982 to 1997 and decreased since 1998 due to a significant reduction in the southern hemisphere. Yao et al. (2012) found that the global land ET increased from 1984 to 2007 in satellite observations, but in fact, the significant increasing trend disappeared after 2000. Mueller et al. (2013) found that the global land ET declined from 1998 to 2005. Zhang et al. (2019) used a coupled diagnostic biophysical model to estimate 8-day global ET at 500-m resolution from July 2002 to December 2017, finding a significant increase in global ET over the past 15 years. Based on the above findings, it is not difficult to speculate that there are complex trends in global land ET during 1982–2017, with the specific performance increasing first then decreasing, finally recovering increase. Zhang et al. (2015a) discovered that the decreasing trend of global terrestrial ET from 1998 to 2008 was an accidental phenomenon, with subsequent recovery of the increasing trend after 2008 by a long-term remote sensing-based land ET record of 1982–2013. However, we would be cautious about concluding on trends from short-time series. Douville et al. (2012) noted that the trend of global land ET should be long term and could not be assessed with short-term data.

In recent years, there are also several studies on the spatio-temporal variations of land ET over China, with different variation trends attributed to the discrepancies in the forcing data and model algorithms. During 1979–2015, most researches showed increasing trends as a whole in China. Combining the Normalized Difference Vegetation Index (NDVI) with climatic data in a physical ET model, Mo et al. (2015) investigated the land ET in China during 1981–2010, and an increasing ET trend was found through the 1980s to mid-1990s, followed by a declining trend. Mao and Wang (2017) calculated grid-averaged ET for the MPM and reanalysis ET for China during 1982–2013 and then compared with the water balance ET values, finding ET datasets showing significant or weak increasing trends with varying increases in amplitude. Bai and Liu (2018) evaluated three global high-resolution ET products across China during 1982–2013; the results indicate that all of them show a consistently increasing trend in most areas of China. Liu et al. (2016) suggested that vegetation greening has increased annual ET while vegetation browning has reduced annual ET in China from 2000 to 2014, using a process-based ecosystem model and a satellite-derived leaf area index (LAI) dataset. However, Mao et al. (2016) found that after taking the change in terrestrial water storage due to reservoir construction into account, the trend of ET decreased to almost zero from 1997 to 2014 in China by quantifying reservoir effects on the estimated ET.

The land ET consists of several different components, including transpiration, bare-soil evaporation, interception loss, open-water evaporation, and sublimation (Miralles et al. 2011a). It is of significant interest to quantify the relative

importance of different components to better understand the underlying dynamics of ET changes in the warming climate. However, there are quite few studies of the different ET components over China. Zhang et al. (2011) used the Soil and Water Integrated Model (SWIM) to simulate the different ET components during 1997–2003 in the upper reaches of Jingjiang River Basin, where bare-soil ET amounts to 259 mm, transpiration amounts to 157 mm, and canopy interception amounts to 27 mm year. Gong et al. (2007) used the soil water balance method and sap flow plus micro-lysimeter methods to estimate ET for 2 years within an apple orchard in northwest China, where bare-soil evaporation dominated in spring and autumn and transpiration became more significant in summer. Lin et al. (2012) observed the ET components at the southeastern fringe of the Qinghai-Tibet Plateau from April to October in 2009; soil evaporation was observed to account for 6% of the total ET, vegetation transpiration for 19% and interception evaporation for 75%, respectively. However, these studies did not show the long-term trend of different components due to the limited study period. There is the need for more studies on the long-term trends of land ET and its components over China for a better understanding of the water cycle changes in the recent decades.

Recently, Miralles et al. (2011b) developed an algorithm to maximize the recovery of ET from current satellite observations and separately estimates the different components of land ET, which is termed Global Land Evaporation-Amsterdam Methodology (GLEAM). The long-term land ET products derived from GLEAM algorithm have been widely validated worldwide and used in the research areas of hydrology (Greve et al. 2014; Miralles et al. 2014a), meteorology (Miralles et al. 2014b; Guillod et al. 2015), and climate extremes (Yang et al. 2015). At present, there is no verification of GLEAM ET in the Yangtze River Basin; however, Yang et al. (2015) have performed the validation in the Huai River Basin, which borders the middle and lower reaches of the Yangtze River valley. The topography and climate in the Huai River Basin is similar to that of the Yangtze River valley. Besides, some verifications indicate GLEAM performs well in China. Bai and Liu (2018) evaluated ET products at the site scale with eddy covariance-based observations in China, finding that GLEAM shows the best consistency with the point observations. Yang et al. (2017) performed ground-based validation and concluded that GLEAM ET over different time scales could estimate actual ET with reasonable accuracy.

Affected by the Asian monsoon, the Yangtze River valley has experienced several serious flood disasters in the past few decades since the spatial and temporal distributions of land water storage are significantly different. With increased population and rapid economic and agriculture development, it makes sense to select the Yangtze River valley, the largest drainage basin in China, as the study area. In addition, hydrological data

here have been obtained, which can support the study with effect. There are a few researches on the long-term trend of actual ET in the Yangtze River valley. Zhou et al. (2016) calculated average ET over the Yangtze River valley by using the GRACE satellite-based measurements as well as the ground-based observations, showing that the ET of the seven sub-catchments was rising with the increasing temperature except for the Poyang Lake and Dongting Lake. Among them, the researches on ET components are few. In consequence, the spatiotemporal variations of total ET and its components, and the dynamics behind the variations, need to be studied to understand the climate change impact on terrestrial water cycle. In this study, we have validated the GLEAM satellite assimilation product in the Yangtze River valley using the water balance method, and then analyzed the changes of actual ET and its different components for the period 1980–2014. Their relations with precipitation, air temperature, and solar radiation are also analyzed and discussed in the context of the warming climate, further identifying the most significant impact factor of ET.

2 Study area, data, and methods

2.1 Study area

The Yangtze River, located in the Central China (90° 33′–122° 25′ E, 24° 30′–35° 45′ N), is the largest river in China, and the third largest in the world. The Yangtze River valley covers an area of 1.8 million km², with a population of roughly 400 million, accounting for one-third of the total population in China. It is the most developed area in China and thus occupies the most important strategic position for the allocation of water resources to support eco-socially sustainable development.

The river originates from the Tibet Plateau and is about 6300 km in length. The topography of the Yangtze River valley is rather complex, and the terrain is depicted as a multi-level ladder, which is shown in Fig. 1. The Yangtze River valley, especially the middle and lower reaches, features a subtropical summer monsoon climate with most precipitation occurring in summer. Precipitation is not evenly distributed across the valley; there is about 200–800 mm in the upper reaches and 800–1600 mm in the middle and lower reaches per year. Precipitation is the main supplier of runoff in the valley, and land ET is one of the important factors that affect the water balance.

The GLEAM ET product has been validated with ET which is derived from water balance method in the Yangtze River valley during the study period of 1980–2000. Considering the availability of hydrological data, 12 river basins in the Yangtze River valley are selected for the validation purpose, which are shown in Fig. 1. For each basin, the river runoff data measured at the basin outlet are used. The used

basins in the Yangtze River valley are shown in Fig. 1, and the locations of hydrological stations, as well as their drainage areas, are listed in Table 2.

2.2 Data

2.2.1 GLEAM data

Currently, there are several land ET products based on FLUXNET observations (Wang and Dickinson 2012), meteorological reanalysis (Simmons et al. 2007), and harmonized data from multiple sources (Jung et al. 2009). Some of the methods of ET estimation are based entirely on empirical statistics (Jime et al. 2009), while others are effectively incorporated traditional estimates based on physical processes (Mu et al. 2011). In the recent years, the land ET estimated with remote sensing technology has received more and more attention due to its large-scale coverage and fine resolutions (Miralles et al. 2011a).

The GLEAM algorithm is a data assimilation methodology rather than deriving land ET directly from satellite imageries. Satellite observations of net radiation, air temperature, precipitation, vegetation optical density, and snow water equivalents are used to derive global land ET in this algorithm. The GLEAM ET product has been validated over the globe using the in situ observations from the eddy covariance instrument (Miralles et al. 2011b), which have suggested the GLEAM ET product can be used to describe the land ET of different ecosystems. The GLEAM algorithm estimates not only the total land ET but also separately estimates its different components of vegetation transpiration, bare-soil evaporation, interception loss, open-water evaporation, and sublimation based on the physical processes (Priestley and Taylor 1972). Except for the GLEAM ET product, so far, there is no other long-term dataset available that consists of different components of land ET. The version of this data is 3.0a and spans a 35-year period through 1980 to 2014, gridded with a spatial resolution of 0.25°, and is available from <https://www.gleam.eu/>. The readers are referred to Miralles et al. (2011b) for detailed descriptions of the GLEAM algorithm for producing this data.

2.2.2 Precipitation, temperature, solar radiation, runoff, FLUXNET ET, and NDVI data

For the analysis of associated dynamics, the Multi-Source Weighted-Ensemble Precipitation (MSWEP) data, ERA-Interim 2-m temperature data, and ERA-Interim surface net solar radiation data are used. MSWEP data have a 3-h temporal and a 0.25° spatial resolution (Beck et al. 2017). ERA-Interim 2-m temperature and surface net solar radiation data have a daily temporal and a 0.25° spatial resolution, which can be downloaded from <https://www.ecmwf.int/>. The meteorological observations of precipitation and temperature

are also used to calculate the ET by water balance method and budyko method. The official products of daily precipitation and air temperature are obtained from China Meteorological Administration, which are gridded with a spatial resolution of 0.5° from meteorological observations of 2472 stations throughout China. River runoff data spanning the period 1980–2000 are provided by the Changjiang Water Resources Commission of the Ministry of Water Resources, which consist of daily records of 12 gauging stations in the Yangtze River valley, which can be downloaded from <http://www.cjw.gov.cn/>. Latent heat flux (LE) data at one eddy covariance tower sites have been obtained from FLUXNET (<http://fluxnet.fluxdata.org/>). We have also used GIMMS NDVI3g data from the Global Inventory Modeling and Mapping Studies (GIMMS) in our study (Pinzon and Tucker 2014).

2.3 Methods

2.3.1 Water balance method

To validate GLEAM ET product in the Yangtze River valley, the water balance method has been used, which has been widely applied over river basins (Senay et al. 2011). For a basin, the actual ET is worked out from the water balance equation:

$$P - ET_W - Q - \Delta\theta = \mu \quad (1)$$

where P is precipitation, ET_W is actual ET estimated from the water balance method, and Q is runoff; $\Delta\theta$ is the change of water storage, which includes changes in soil moisture, groundwater storage, snow cover and ice, lakes, reservoirs, and rivers. μ is the discrepancy of the water balance, which should be zero when all components are measured accurately. In this study, we estimate the basin-wide water balance based on multiple year averages. $\Delta\theta$ is generally small and thus ignored when the water balance is computed for annual values and for multiple years (Senay et al. 2011). μ is the divergence from zero which is the net cumulative error of all measurements (Dooge 1975), which is also considered to be zero.

2.3.2 Budyko framework

Budyko framework is a simple and intuitive method to estimate ET at the steady state, where the average annual evapotranspiration ratio is assumed to be a function of dryness (Wang and Zhou 2016). Considering the impacts of catchment properties, the formula has been improved as follows (Fu 1981):

$$ET_B = P \left(1 + \frac{E_0}{P} \left[1 + \left(\frac{E_0}{P} \right)^{\omega} \right]^{1/\omega} \right) \quad (2)$$

where ET_B represents actual ET, P is precipitation, and E_0 is potential ET; w is a parameter representing the catchment conditions such as soils and vegetation. Fu's equation has been widely used in the last decade (Zhang et al. 2008, Greve et al. 2015).

To validate the relationship between GLEAM ET and ET_W , as well as ET_B , we use the error metrics of Pearson correlation coefficient (R), $BIAS$, $RBIAS$; mean absolute error (MAE), $RMAE$; and root mean square deviation ($RMSD$), $RRMSD$. The statistic values are defined as follows:

$$R = \frac{\sum_{i=1}^n (G_i - \bar{G})(W_i - \bar{W})}{\sqrt{\sum_{i=1}^n (G_i - \bar{G})^2} \sqrt{\sum_{i=1}^n (W_i - \bar{W})^2}} \quad (3)$$

$$BIAS = n^{-1} \sum_{i=1}^n (G_i - W_i) \quad (4)$$

$$RBIAS = \frac{BIAS}{\bar{W}} \quad (5)$$

$$MAE = n^{-1} \sum_{i=1}^n |G_i - W_i| \quad (6)$$

$$RMAE = \frac{MAE}{\bar{W}} \quad (7)$$

$$RMSD = \sqrt{n^{-1} \sum_{i=1}^n (G_i - W_i)^2} \quad (8)$$

$$RRMSD = \frac{RMSD}{\bar{W}} \quad (9)$$

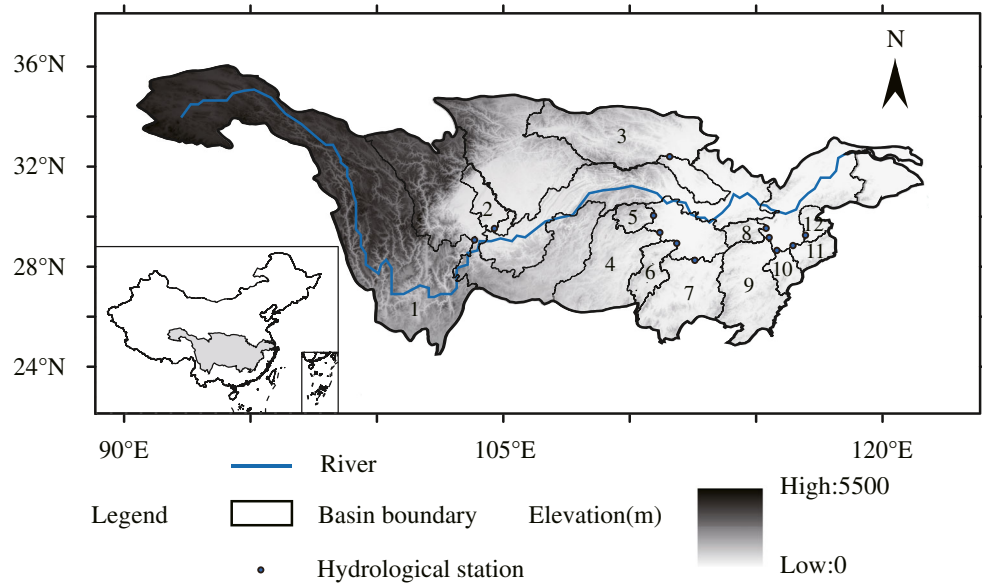
where n represents the sample size; G_i and W_i respectively represent the ET data from GLEAM product and water balance method (or Budyko method) at time i . \bar{G} and \bar{W} represent the average of G_i and W_i .

2.3.3 Theil-Sen slope

A nonparametric statistic of Theil-Sen slope is used to determine the linear trend of land ET and its different components, respectively. Prior to the linear regression, the Theil-Sen slope is insensitive to outliers and thus leads to robust estimation of linear trend in the data under investigation. It can show more accurate skewness within the data than the simple linear regression and is also comparable to the least squares method for a normal distribution data. It is considered as the most robust nonparametric technique for estimating linear trends and has been widely used in studies of hydrology (Zamani et al. 2017) and meteorology (Shi et al. 2016).

As defined by Theil (1950), the slope of a set of two-dimensional points (x_i, y_i) is the median of the slope $(y_j, y_i)/(x_j, x_i)$ determined by the sampling points of all pairs. Sen (1968) extended this definition to deal with the situation

Fig. 1 The location and topography of the Yangtze River valley in China, as well as the locations of hydrometric stations. The numbers in the basins are their respective IDs, which are consistent with those in Table 2 and Fig. 2. The basins are (1) Jinsha river basin, (2) Mintuo river basin, (3) Hanjiang basin, (4) Yuan river basin, (5) Lishui basin, (6) Zijiang basin, (7) Xiangjiang basin, (8) Xiushui basin, (9) Ganjiang basin, (10) Fu river basin, (11) Xinjiang basin, (12) Raohe basin



where two data points have the same x -coordinates. In this study, the linear trends of land ET and its components are calculated with the following formula of the Theil-Sen slope:

$$\Delta = \text{median}\left(\frac{x_j - x_i}{j - i}\right) \tag{10}$$

where median represents the median function; x_i and x_j represent the data at time i and j . In a statistical sense, Δ means the averaged variation of the change in time between time steps. If $\Delta > 0$, the trend is increasing; if $\Delta < 0$, the trend is decreasing.

2.3.4 Mann-Kendall trend test

Mann-Kendall test is a nonparametric statistical method which is widely used to determine the significance of linear trend in a data sequence (Modarres and Paulo 2007). It does not require the samples to follow a certain distribution, and it is not disturbed by a small number of outliers. Many studies have used the Mann-Kendall method to quantify the significance of temporal trends in hydro-meteorological time series (Ribeiro et al. 2015). The statistic of Mann-Kendall (S) is calculated as:

$$S = \sum_{i=1}^{n-1} \sum_{j=i+1}^n \text{sgn}(x_j - x_i) \tag{11}$$

In the above formula, n represents the number of data points; x_j and x_i represent the data at time j and i ; and $\text{sgn}(x_j - x_i)$ is a sign function as:

$$\text{sgn}(x_j - x_i) = \begin{cases} +1 & \text{if } x_j - x_i > 0 \\ 0 & \text{if } x_j - x_i = 0 \\ -1 & \text{if } x_j - x_i < 0 \end{cases} \tag{12}$$

The variance is computed as:

$$\text{Var}(S) = \frac{n(n-1)(2n+5) - \sum_{i=1}^m t_i(t_i-1)(2t_i+5)}{18} \tag{13}$$

where m represents the number of tied groups and t_i refers to the number of ties of extent i . A tied group means a set of sample data with the same value. In cases where the sample size $n > 10$, the standard normal test statistic Z_S is computed using the following equations:

$$Z_S = \begin{cases} \frac{S-1}{\sqrt{\text{Var}(S)}}, & \text{if } S > 0 \\ 0, & \text{if } S = 0 \\ \frac{S+1}{\sqrt{\text{Var}(S)}}, & \text{if } S < 0 \end{cases} \tag{14}$$

If Z_S is positive, the trend is increasing while negative one shows decreasing trends. Testing trends is done based on the specific α significance level. When $|Z_S| > Z_{1-\alpha/2}$, the null hypothesis is rejected then a significant trend exists in the time series, of which $Z_{1-\alpha/2}$ is obtained from the standard normal distribution table. In this study, significance level $\alpha = 0.05$ was used.

3 Results

3.1 Validation of GLEAM ET

We have calculated the monthly FLUXNET ET data (generally reflected by latent heat flux) with the following equation

from Qianyanzhou site during 2003–2005 to evaluate the product:

$$ET = \frac{LE}{\lambda} \quad (15)$$

where LE represents latent heat flux, λ is a fixed value of 2.45 MJ/kg.

The profiles of the selected FLUXNET site have been listed in Table 1. Figure 2a shows the scatter plot of the GLEAM and the FLUXNET ET data, together with the overall statistics of used error metrics. The RMSD is 16.48 mm month, MAE of 24.21 mm month, and BIAS of 24.21 mm month. Compared with FLUXNET ET, although there is an overestimation in the whole valley, as can be seen in Fig. 2a, there is a good correlation between them.

The annual values of the GLEAM ET and the ET_W estimations from the water balance method for the 12 basins listed in Table 2 have been averaged during 1980–2000. It is apparent that the differences between GLEAM ET and ET_W vary widely among different basins. It appears in most basins that the GLEAM data have overestimated the total ET compared to the ET_W , except for two of them. The differences are relatively small in the basins of Hushan, Taojiang, Xiangyang, Shimen, Xiangtan, Lijiadu, Waizhou, and Taoyuan, which are mainly located in the middle reaches of the Yangtze River valley. The differences appear relatively large in the basins of Lijiawan, Pinshan, Qiujin, and Meigang.

Figure 2b shows the scatter plot of the GLEAM and the ET_W data, together with the overall statistics of used error metrics of R , $BIAS$, MAE , and $RMSD$. The GLEAM ET data is regressed on the ET_W data, and the 1:1 line is also depicted. A good linear relationship is found between both data and their correlation coefficient appears to be 0.74, indicating they are consistent in general. Overall, the $RMSD$ is 101.84 mm/year. Although there is a general overestimation in GLEAM ET with an MAE of 77.33 mm/year and a $BIAS$ of 56.90 mm/year, they are less than 10% of the total ET_W across the analyzed 12 basins, which are within the acceptable error ranges. There are two basins, namely the Qiujin and the Meigang basins, which show large MAE of 185.4 mm and 226.3 mm/year, respectively; this might be partly due to their smaller drainage areas. Therefore, the GLEAM ET is appropriate for further analysis. Similarly, Fig. 2c shows the scatter plot of the GLEAM and the ET_B data, together with the overall statistics of used error metrics of R , $BIAS$, $RBIAS$, MAE , $RMAE$, $RMSD$, and $RRMSD$. The $RMSD$ is 159.79 mm year, MAE of 133.19 mm year, and $BIAS$ of

128.05 mm year. Compared with ET_B , there is a general overestimation in GLEAM ET.

3.2 Seasonal variations

3.2.1 Variations of total ET

We first show in Fig. 3 the spatial distributions of the annual mean values of total ET and those in each season, which are obtained from the study period of 1980–2014. Figure 3a shows the annual ET, and Fig. 3b–e show those for spring, summer, autumn, and winter, respectively. We can see from Fig. 3a that the amount of annual ET is not evenly distributed in space over the Yangtze River valley. It gradually increases from the upper reaches to the middle and lower reaches of the Yangtze River valley. In the upper reaches, the annual ET amounts to less than 600 mm year; at the source area of the Yangtze River over the Tibetan Plateau, the amount of annual ET is less than 400 mm year. In the middle and lower reaches, the annual ET amounts to more than 700 mm year; particularly, it amounts to more than 900 mm year in the Poyang Lake basin.

The ET shows significant spatiotemporal variations among seasons. In spring, the ET amounts to 150–250 mm in most areas of the Yangtze River valley. In the source area of the Yangtze River on the Tibetan Plateau, the total ET in spring is even less 100 mm. In summer, the ET amount is much higher than those in the other seasons. It increases to an amount of about 300 mm in the upper reaches, and 300–350 mm in the lower and middle reaches. In autumn, the total ET is reduced to 150–200 mm in the middle and lower reaches, and even less in the upper reaches. In winter, the total ET is further reduced to less than 100 mm throughout the valley. The total ET exhibits much stronger seasonal variations in the middle and lower reaches than that in the upper reaches. That is because the middle and lower reaches of the Yangtze River basin is dominated by the East Asian Summer Monsoon system, which brings abundant precipitation in the summer seasons (Lv et al. 2004).

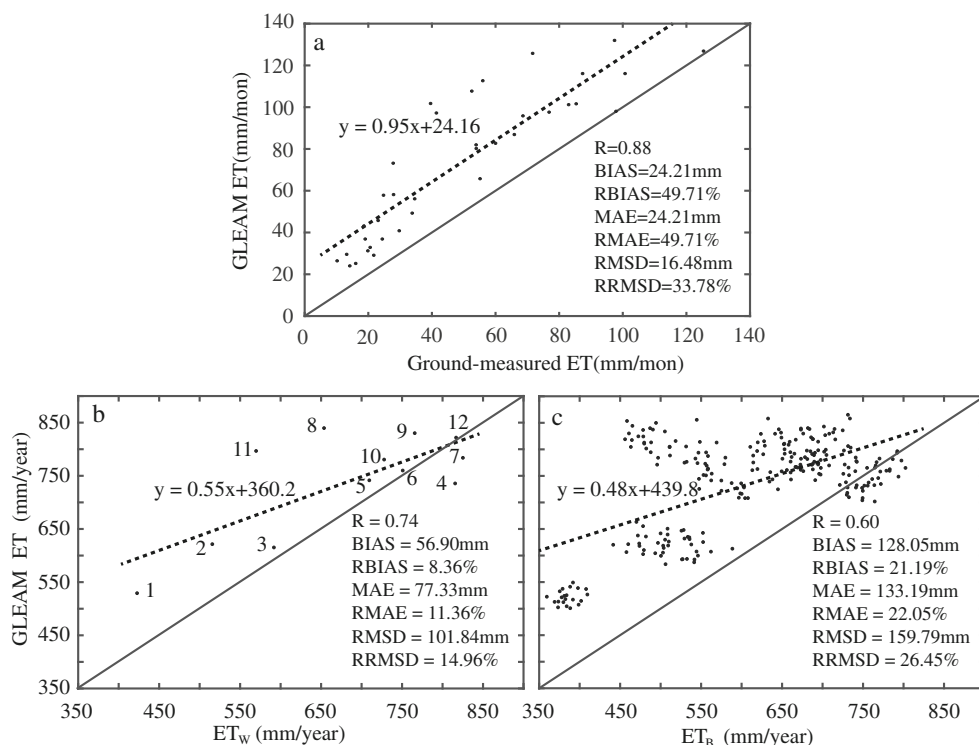
3.2.2 Variations of ET components

Looking into the variations of the different ET components helps our understanding of the underlying dynamics of the ET changes. In Fig. 4, we show the annual amounts of each ET component in the Yangtze River valley, including vegetation transpiration, bare-soil evaporation, interception loss, and

Table 1 Profiles of the selected FLUXNET site for validation in the Yangtze River basin

Site name	Longitude (°E)	Latitude (°N)	Altitude	Time span	IGBP biomes
Qianyanzhou	117.269	28.908	110.8	2003–2005	ENF

Fig. 2 Comparisons between FLUXNET ET, ET_w , ET_b , and GLEAM ET for the 12 basins of the Yangtze River valley. The 1:1 line is depicted



open-water evaporation. The annual amount of each component is derived from the multiple-year average within the study period of 1980 and 2014.

Similar to the total ET, the amount of annual transpiration shows significant spatial heterogeneity which gradually increases from the upper to the middle and lower reaches (Fig. 4a). Large-scale transpiration is principally controlled by soil water content, vegetation, and temperature. In the middle and lower reaches, the annual transpiration amounts to 500–600 mm per year, where there is rich vegetation and precipitation. The amount of transpiration is particularly large, amounting to more than 600 mm per year, in the Poyang Lake basin where there are densest vegetation, maximum precipitation, and highest temperature. In the river source areas, the annual transpiration amounts to only 100–200 mm or even less, jointly determined by the limited vegetation, precipitation, and also temperature.

The canopy interception loss appears to be quite complex in terms of its spatial pattern (Fig. 4b), which is significantly different from vegetation transpiration. The determinants of canopy interception loss involve precipitation, vegetation density, and also canopy types from different vegetation species. The complex spatial pattern of interception loss in the Yangtze River valley is suggested to be more affected by vegetation. There are the most interception losses in the Poyang Lake and the Dongting Lake basins reaching around 160 mm year, where the land is densely covered by broad leaf plants and trees. Distinctively, there appears much less interception in the Sichuan basin than the surrounding areas, which is in a rather good agreement with the vegetation distributions there. The

Sichuan basin is a well-developed agricultural area where the land is mostly used for crops; however, the surrounding areas of the basin are mostly mountains and covered by forests of which the canopy is more capable of intercepting precipitation than crops. In most of the other areas, the interception loss is below 40 mm year. The bare-soil evaporation is limited to 60–100 mm year in most areas of the Yangtze River valley (Fig. 4c). In the middle reaches, the bare-soil evaporation is particularly limited, amounting to only around 60 mm year. There is more bare-soil evaporation in the river source area on the Tibetan Plateau where the vegetation is relatively sparse, and the amount reaches about 140 mm year.

It is important to determine the dominant ET component in each grid cell so as to understand their respective contributions in the terrestrial water cycle. Figure 4e shows the dominant component and its percentage of total ET in the Yangtze River valley averaged during the study period. Obviously, the above results have shown that transpiration is a predominant component of the land ET in the Yangtze River valley, except for the source regions and large water bodies, with the values larger than 65%. It indicates that changes of transpiration provide a significant understanding into biological feedbacks onto the atmosphere. It may also provide meritorious information for restraining model predictions of future change. Therefore, the biophysical processes are indicated to be an essential player in the land water cycle.

We have shown in Fig. 5 the seasonal amount of different ET components in the Yangtze River valley during the study period of 1980–2014. The first row shows the amount of

Table 2 Profiles of the selected 12 hydrological stations for validation in the Yangtze River basin

Station name	ID	Longitude (°E)	Latitude (°N)	Drainage area (10^4 km ²)	ET _w (mm/year)	GLEAM ET (mm/year)
Pinshan	1	104.166	28.644	45.67	423.0	528.8
Lijiawan	2	104.967	29.133	2.30	515.9	621.0
Xiangyang	3	112.150	32.031	13.04	592.0	614.8
Taoyuan	4	111.483	28.900	11.01	815.8	735.2
Shimen	5	111.384	29.588	1.95	709.8	741.1
Taojiang	6	112.125	28.528	3.45	751.1	759.5
Xiangtan	7	112.926	27.866	10.27	825.4	783.4
Qiujiu	8	115.680	29.163	1.33	653.9	839.3
Waizhou	9	115.840	28.633	8.32	765.9	829.8
Lijiadu	10	116.161	28.215	1.57	728.1	780.1
Meigang	11	116.818	28.438	1.54	570.0	796.3
Hushan	12	117.269	28.908	1.19	817.0	821.4

transpiration in four seasons. In spring, it is between 90 and 210 mm in most areas of the Yangtze River valley, relatively less in the source region. In summer, transpiration increases rapidly, reaching the amount of 150–270 mm in most areas,

mainly due to the increases in air temperature and monsoonal precipitation, as well as the recovery of vegetation. With temperature dropping and precipitation reduced for the withdrawal of summer monsoon in autumn, transpiration is reduced to

Fig. 3 The multiple-year annual and seasonal land ET for the period 1980–2014 in the Yangtze River valley (unit: mm). **a** Whole year. **b** Spring. **c** Summer. **d** Autumn. **e** Winter

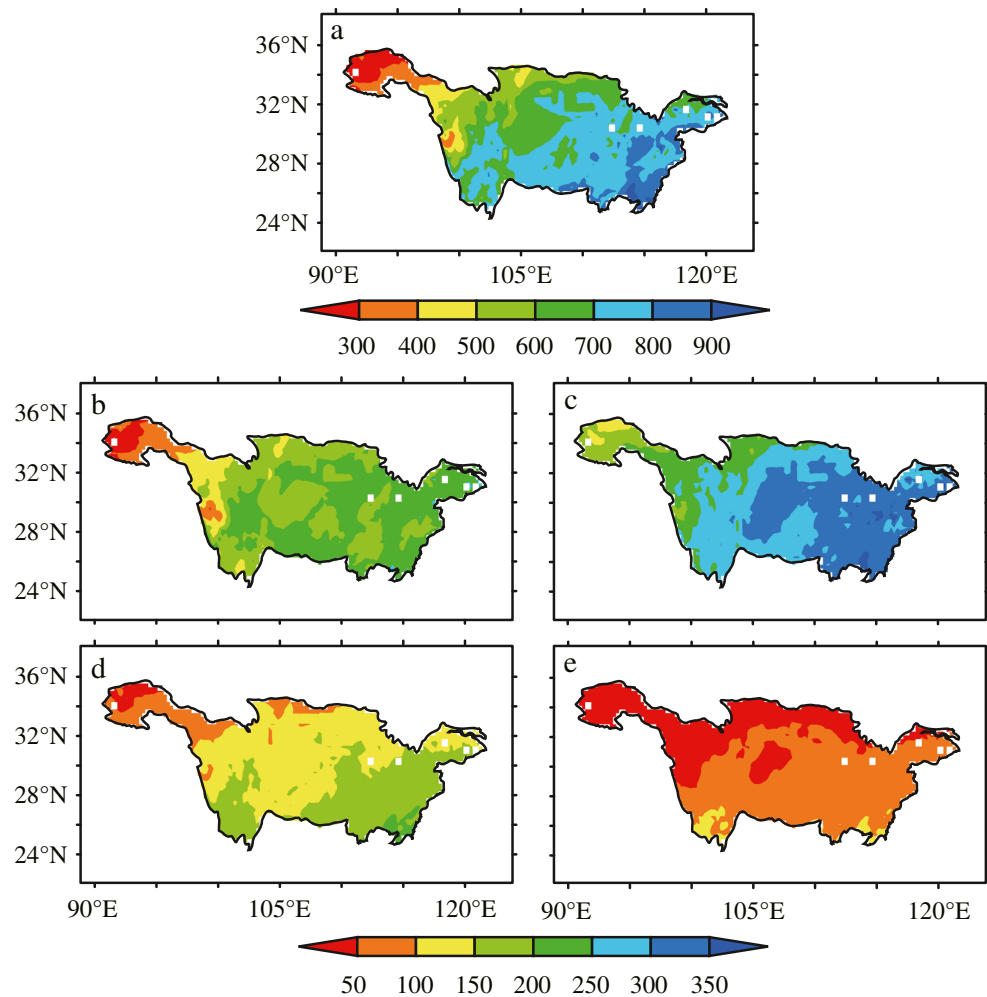
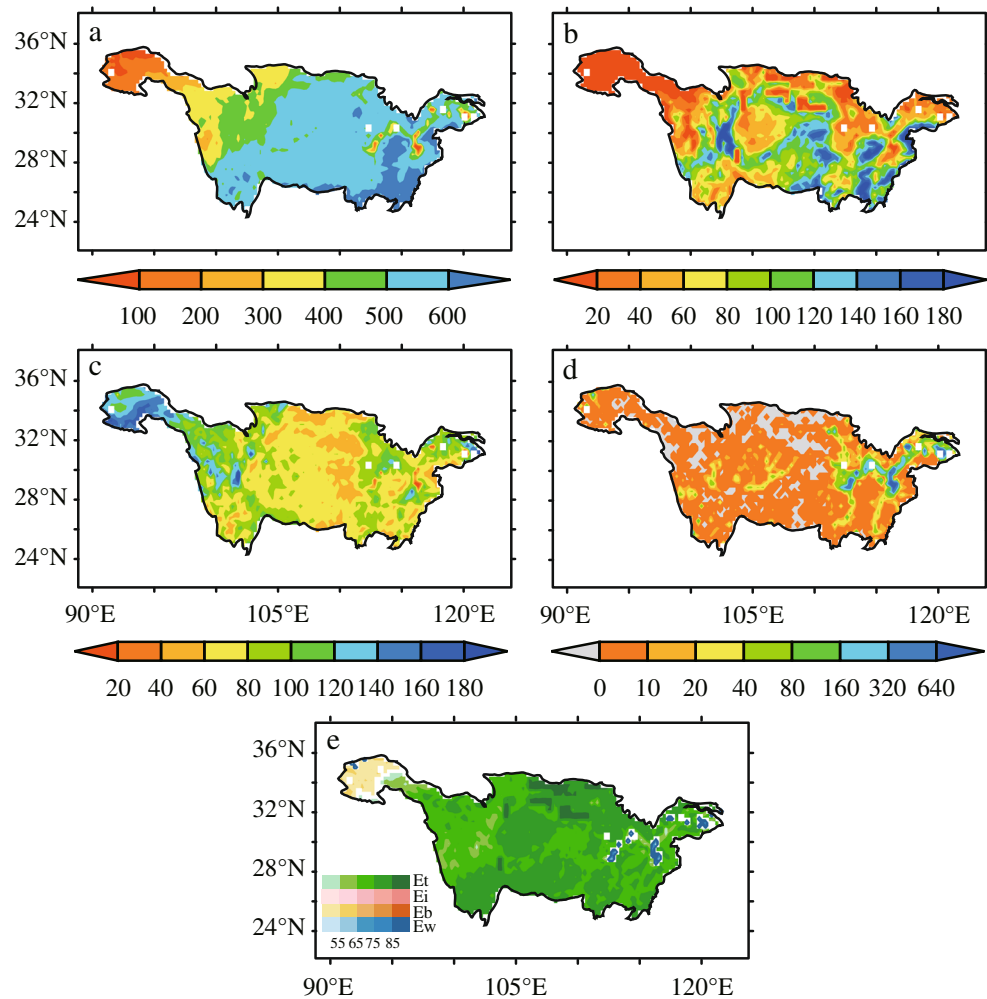


Fig. 4 The annual amount of different components of total ET in the Yangtze River valley during 1980–2014 (unit: mm). **a** Transpiration. **b** Canopy interception. **c** Bare-soil evaporation. **d** Open-water evaporation. **e** The percentage of dominant ET component (unit: %)



about lower than 90 mm in the upper reach and about 90–210 mm in the middle and lower reaches. While in winter, all of precipitation, temperature, and vegetation canopy drop to their minimums, transpiration is reduced to its minimum of less than 90 mm over the Yangtze River valley.

As shown in Fig. 5b, the spatial patterns of interception loss are relatively similar from spring to autumn. There is less interception loss in the Sichuan Basin than in surrounding mountain areas due to different vegetation types as mentioned above, which is an obvious spatial structure. The interception loss in the surrounding mountain areas reaches its maximum more than 45 mm with maximum precipitation in summer. Bare-soil evaporation occurs mainly in areas where vegetation is relatively sparse and soil is humid. In spring, the bare-soil evaporation is, to some extent, evenly distributed with an amount of 10–30 mm over the Yangtze River valley. In summer, it generally increases to 20–40 mm with increased precipitation in most areas and reaches more than 50 mm in the source regions which is particularly significant. In the central and the eastern parts of the Yangtze River Valley, less bare soil resulted from the vegetation recovery offsets the increase of

bare-soil evaporation caused by increased precipitation. However, in the source regions, though there is a slight increase in precipitation, the vegetation is relatively sparse in all seasons, leading to a rapid increase in bare-soil evaporation. In autumn and winter, the bare-soil evaporation is reduced to lower than 30 mm and 15 mm respectively in most areas of the Yangtze River valley. On account of originating from large water bodies of lakes and rivers, the open-water evaporation maintains the same spatial patterns with distinct structures in all seasons around the Poyang Lake, the Dongting Lake, and the Yangtze River downstream. From spring to autumn, it amounts to 80–160 mm in these areas, while in winter, it is reduced to 20–80 mm due to the drop in temperature.

3.3 Long-term trends

3.3.1 Trends of total ET

To understand the spatial distributions of the ET trends, we show in Fig. 6 the pixel-wise linear trends of the ET in the Yangtze River valley for the period 1980–2014. Figure 6a

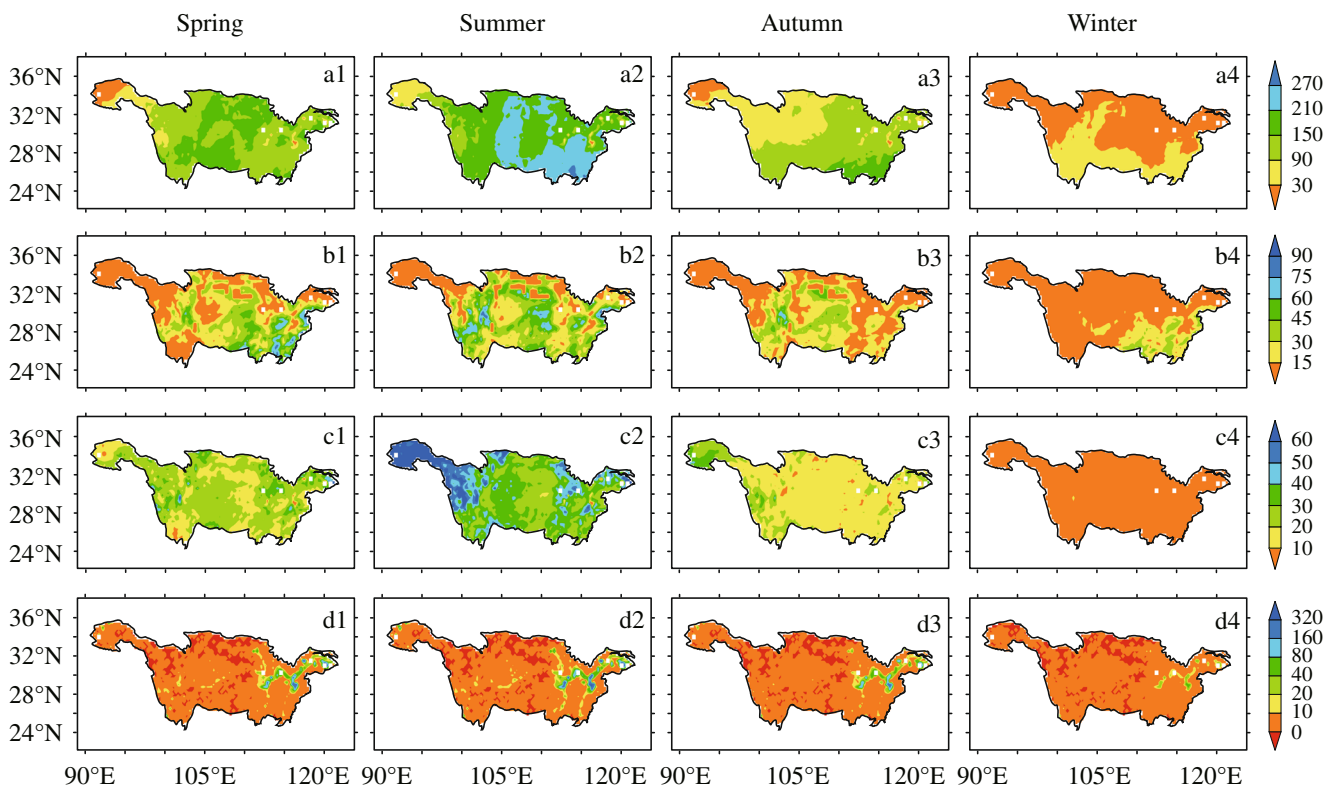


Fig. 5 The seasonal amount of different components of total ET in the Yangtze River valley during 1980–2014 (unit: mm). (a1–4) Transpiration, (b1–4) canopy interception, (c1–4) bare-soil evaporation, (d1–4) open-water evaporation

shows the linear trends for the annual ET, and Fig. 6b–e show those for the separate seasons. There appears to be a significant spatial heterogeneity for the trends of annual ET. As shown in Fig. 6a, there are significant trends in the annual ET, passing significance test at 0.05 level, in the middle and lower reaches of the Yangtze River valley, reaching 20–30 mm/10a. However, there are no significant trends, increasing or decreasing, observed in most areas of the upper reaches, except for the river source areas on the Tibetan Plateau. In spring, the total ET shows a quite similar spatial pattern with significant increasing trends in the middle and lower reaches, which are about 4–10 mm/10a. Those increasing trends are particularly stronger in Jiangxi and Anhui Provinces with a rate of 8–10 mm/10a. In summer, there are also increasing trends in the lower and middle reaches, which are of the order as those in spring; however, decreasing trends occur in Sichuan Province with rates of about -6 mm/10a. In autumn, there are also increasing trends observed in most areas of the middle and lower reaches but the rates are kind of reduced to 2–6 mm/10a, and there are no decreasing trends observed. The interannual variations of ET in winter appear to be quite different from those of the other seasons. There are no significant trends observed in most areas of the valley, except for the slight decreasing ones in the upper reaches. Thus, the increased ET in the Yangtze River valley during 1980–2014 is mainly due to its increases in the middle and lower reaches from spring to autumn.

3.3.2 Trends of ET components

Each ET component may have different properties in terms of their long-term trends. Figure 7 shows the spatial distributions of linear trends of each ET component in the Yangtze River valley for the period of 1980–2014, which is expressed in unit mm/10a. As shown in Fig. 7a, transpiration has experienced a significant increasing trend in the middle and lower reaches in the past 35 years, with an increasing rate of more than 20 mm/10a. It is well-understood that vegetation transpiration is jointly determined by precipitation, temperature, and vegetation structure etc. In the past decades, the amount of precipitation shows a decreasing trend in the upper reaches and an increasing trend in the middle and lower reaches of the Yangtze River valley (Su et al. 2004). The Yangtze River valley has actually experienced a greening trend since the 1980s (Peng et al. 2015), and the temperature increase was also statistically significant (Tian and Yang 2017). Thus, the increases of precipitation, vegetation, and temperature may have jointly caused the increased transpiration in the Yangtze River valley. However, there is no significant trend observed for transpiration in most areas of the upper reaches. This spatial pattern of linear trends is quite similar with that of the total ET, due to the fact that transpiration is the predominant component of total ET.

Surprisingly, the canopy interception appears to decrease in most areas of the middle and lower reaches. In the past

Fig. 6 The spatial distributions of linear trends of total ET in the Yangtze River valley for the period 1980–2014. **a** Whole year. **b** Spring. **c** Summer. **d** Autumn. **e** Winter. The unit is mm/10a. The shaded areas have passed the 5% significance test

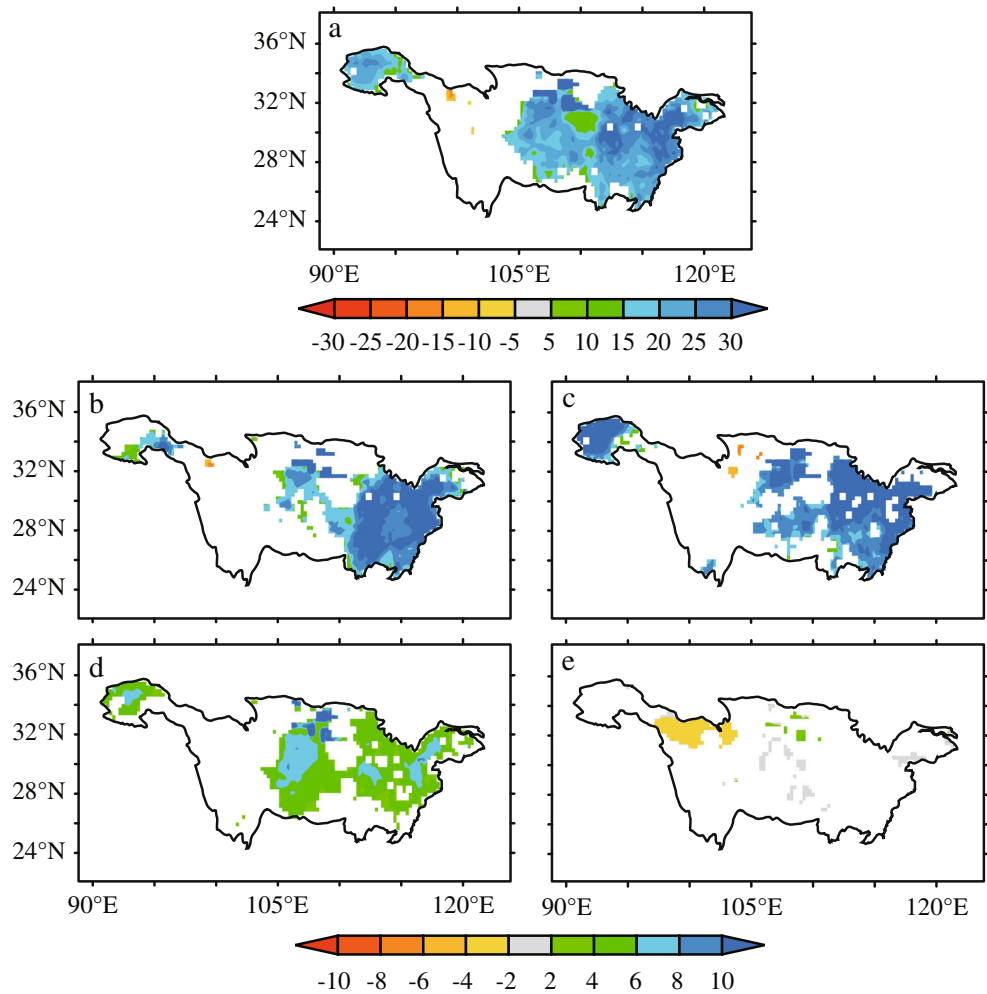
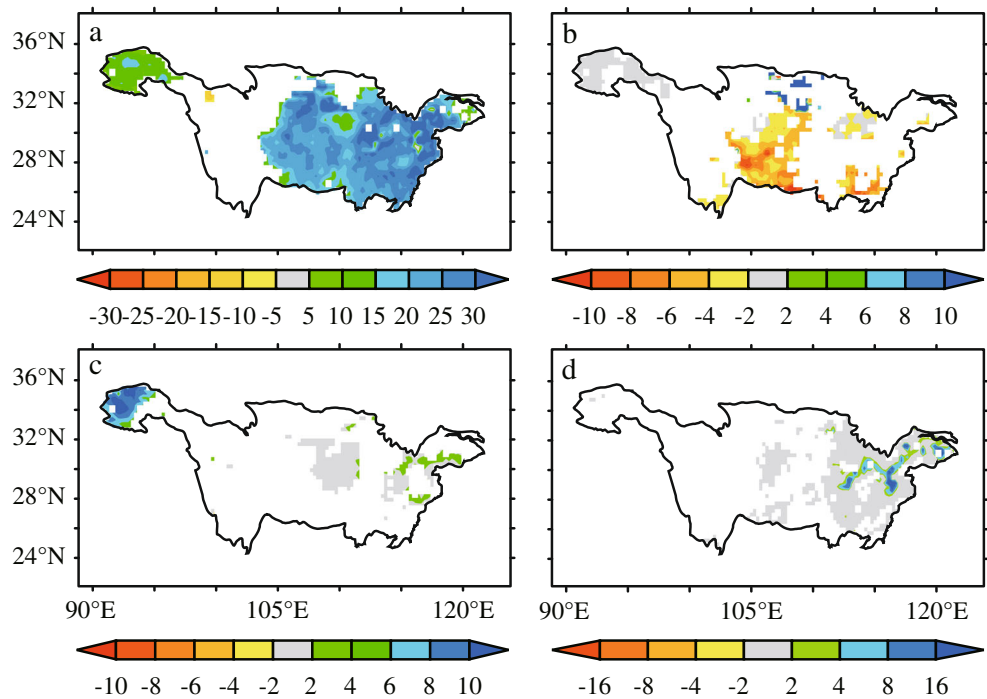


Fig. 7 The spatial distributions of linear trends of each ET component in the Yangtze River valley for the study period of 1980–2014. **a** Transpiration. **b** Canopy interception. **c** Bare-soil evaporation. **d** Open-water evaporation. The shaded areas have passed the 5% significance test



decades, study has revealed that the small precipitation events have decreased in the Yangtze River valley, although the heavy precipitation events have largely increased (Su et al. 2004). It is understandable that canopy interception is more related to small rather than heavy precipitation events, and thus, the decreased small precipitation events may have led to decreased canopy interception. Significant increasing trends of interception only appear in specific regions of Chongqing and Hubei Provinces at the rate of 8–10 mm/10a. To study the effects of heavy and small precipitation events on canopy interception, the rainfall events larger than 95th percentile based on daily precipitation are defined as heavy precipitation, and those less than 10 mm are considered in the analysis of small precipitation (Ali et al. 2013). As shown in Fig. 8a, the variation of heavy precipitation appeared in limited areas; however, small precipitation events (Fig. 8b) decrease in many areas. By contrast, the variation of small precipitation can better explain the change of canopy interception, which means small precipitation events are the main factor leading to the decrease of canopy interception.

As for bare-soil evaporation (Fig. 7c), there are no trends observed in most areas in the Yangtze River valley, except for the river source area on the Tibetan Plateau with an increasing trend of 4–10 mm/10a. The water-body evaporation appears to increase but only at the Poyang Lake, the Dongting Lake, and the Yangtze River downstream, with an increasing rate of 8–16 mm/10a. It is known that evaporation from large water bodies is mainly controlled by near surface air temperature; therefore, the increase in water-body evaporation can be attributed to the warming climate in the recent decades.

3.4 Relations with precipitation, temperature, and solar radiation

3.4.1 Spatial relations

Recently, attentions have been paid to the influencing factors of land ET in the warming climate, considering mainly water supply from precipitation and atmospheric demand of terrestrial flux (Yang et al. 2016). In this study, we have analyzed the

possible dynamics of changes of land ET and its components in the Yangtze River valley, using ERA-Interim 2-m air temperature (T), Multi-Source Weighted-Ensemble Precipitation (MSWEP) data (P), and ERA-Interim solar radiation (R_s) spanning 1980–2014. Two kinds of analysis are made. First, considering the Yangtze River valley is rather large; we have studied the effects of air temperature, precipitation, and solar radiation on the spatial patterns of ET and its components using correlation analysis (R), so as to understand the spatial dynamics. On each pixel, the multiple-year averages of each variable are computed, respectively. Data sequences are constructed with the multiple-year averages on each pixel, to which correlation analyses are then performed. Second, pixel-wise correlation analyses are performed based on the annual values of each variable so as to understand the temporal dynamics. Air temperature, precipitation, and solar radiation may interact with each other, leading to compounding effect on the land ET (Sun et al. 2014). To eliminate this effect, we have also made a partial correlation (PR) analysis in addition. The derived results are shown in Table 3. We note that asterisk in Table 3 indicates the value has passed 1% significance test.

Seen from Table 3, the total ET has strong relations with both air temperature, precipitation, and solar radiation in the Yangtze River valley. The total ET shows very high correlation coefficients (R) of 0.88, 0.86, and -0.62 with air temperature, precipitation, and solar radiation, respectively; the partial correlation coefficients with air temperature and precipitation are reduced to some extent, but are still 0.68 and 0.58. However, the partial correlation coefficients with solar radiation are greatly reduced, with the value of 0.13. Thus, it is indicated that only air temperature and precipitation have significant influences on the spatial pattern of total ET in the Yangtze River valley. Although precipitation is the moisture source, air temperature appears to play a role of the same order as precipitation in spatial patterning of land ET. As for transpiration, the correlation coefficient with temperature is 0.77 and the partial correlation coefficient is largely reduced to 0.35; with precipitation, the correlation coefficient is 0.83 and reduced to 0.51 for partial correlation coefficient; as for solar radiation, the correlation coefficient is -0.62 and largely

Fig. 8 The spatial distributions of linear trends of heavy (a) and small (b) precipitation in the Yangtze River valley for the study period of 1980–2014. The unit is mm/10a. The shaded areas have passed the 5% significance test

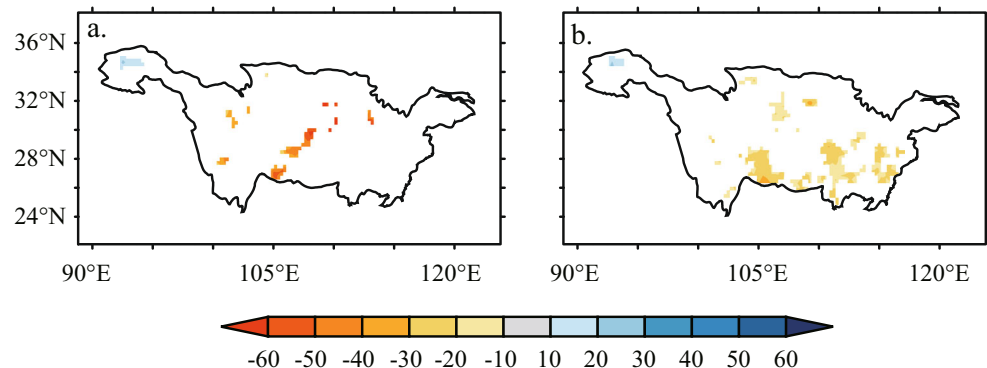


Table 3 The correlation coefficient (R) and partial correlation coefficient (PR) of multiple-year averaged ET and its components with air temperature (T), precipitation (P), and solar radiation (R_s). (Asterisk indicates the value has passed the significance test at 1% level)

		T	P	R_s
R	Total ET	0.88*	0.86*	-0.62*
	Transpiration	0.77*	0.83*	-0.62*
	Interception	0.71*	0.45*	-0.48*
	Bare-soil evaporation	-0.53*	-0.61*	0.58*
	Open-water evaporation	0.09*	0.15*	0.00
PR	Total ET	0.68*	0.58*	0.13*
	Transpiration	0.35*	0.51*	-0.03
	Interception	0.63*	-0.29*	-0.20*
	Bare-soil evaporation	-0.07*	-0.24*	0.24*
	Open-water evaporation	-0.01	0.17*	0.15*

reduced to -0.03 for partial correlation coefficient. This indicates precipitation plays a more important role than air temperature in the spatial patterning of vegetation transpiration, and solar radiation has almost no influence in transpiration. Interception loss shows correlation coefficients of 0.71, 0.45 and -0.48 with air temperature, precipitation and solar radiation, respectively; the partial correlation coefficient with air temperature is slightly reduced to 0.63 and that with precipitation and solar radiation is -0.29 and -0.20. This indicates the spatial patterning of interception loss is mainly controlled by air temperature and has little to do with temperature and solar radiation. As for bare-soil evaporation, we are surprised to find out there are obvious negative correlation coefficients of -0.53 and -0.61 with air temperature and precipitation, respectively and the correlation coefficient between bare-soil evaporation and solar radiation is 0.58. Considering partial correlation coefficients, they are -0.07, -0.24 and 0.24 with air temperature, precipitation and solar radiation respectively. The open-water evaporation shows trivial correlations, as well as partial correlations, with air temperature, precipitation, and solar radiation, indicating limited influences of temperature, precipitation, and solar radiation on evaporation from open water. This makes sense as the locations of water bodies are obviously determined by topography.

3.4.2 Temporal relations

To understand the temporal dynamics of total ET and its components, we have computed their pixel-wise partial correlation coefficients with air temperature, precipitation, and solar radiation respectively using annual values during 1980–2014.

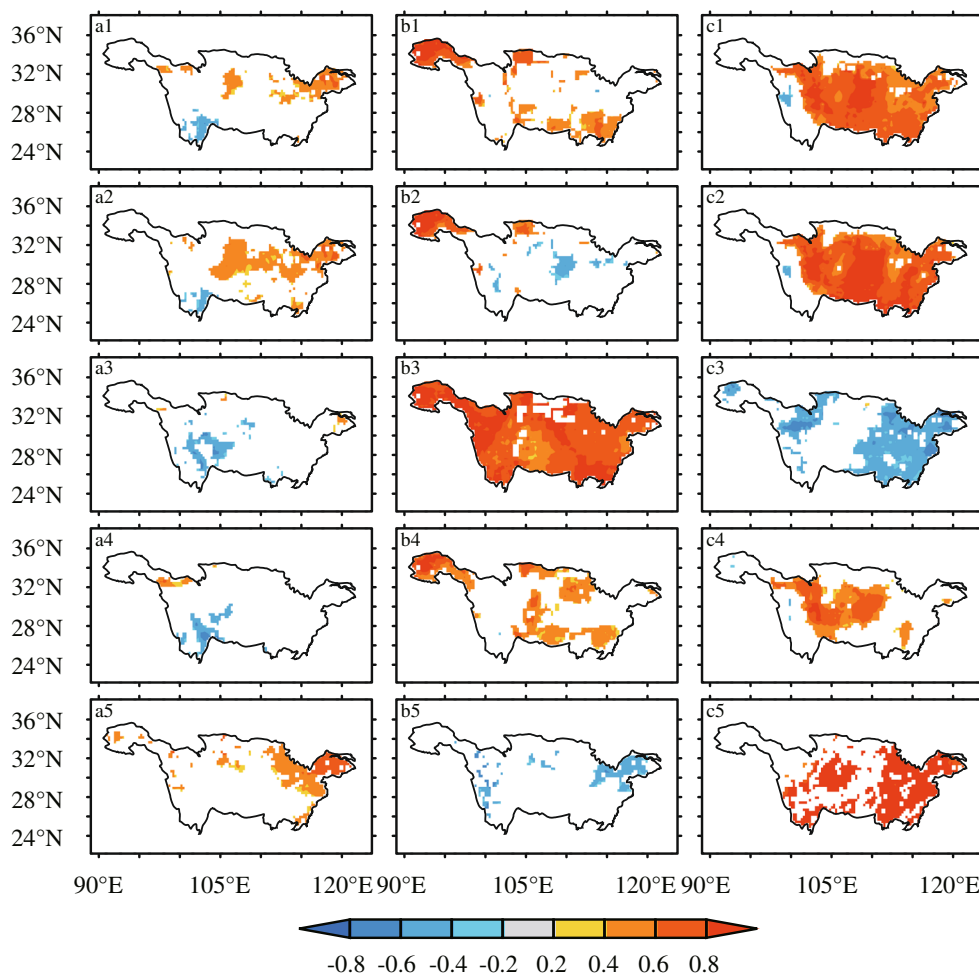
The first column of Fig. 9 shows the derived pixel-wise correlation coefficients between air temperature and total ET, as well as its components in the Yangtze River valley. The second and third columns show those with precipitation and solar radiation. The shaded correlations have passed the 5%

significance test. The total ET appears to have positive correlations with solar radiation in most areas of the valley, with correlation coefficients higher than 0.4. In the source area of the Yangtze River, the correlations coefficients with precipitation have reached values larger than 0.6. It indicates that in most areas, solar radiation is the dominant factor, while precipitation plays the leading role in the source areas. In addition, the effect of air temperature is much weaker than precipitation and solar radiation. The correlations with transpiration appear to have almost the same spatial pattern, with equivalent correlation strengths. Although air temperature is positively correlated with transpiration in some areas, it is still much weaker than solar radiation. This is not surprising as transpiration contributes to a prevailing portion of total ET. As expected, the interception shows strong positive correlations with precipitation throughout the Yangtze River valley. The negative correlations with air temperature are in accord with the result found by Lockwood (1990) that interception loss tended to decrease with increasing temperature from the numerical simulation using a multilayer model pine canopy. However, it is interesting to find the notable negative correlations with solar radiation in large areas of the middle and lower reaches of the Yangtze River valley. We have further calculated the correlation coefficients between precipitation and solar radiation in each grid cell. As can be seen from Fig. 10, solar radiation does show a significant negative correlation with precipitation. What we know is that canopy interception occurs only in rainy days, and possibly, increased clouds on rainy days may reduce solar radiation. Considering bare-soil evaporation, it has positive correlations with solar radiation in most areas of the valley, with correlation coefficients higher than 0.4. While in the source area of the Yangtze River, it has positive correlations with precipitation. It indicates that the dominant factors are similar to transpiration. The open-water evaporation shows significant positive correlations with solar radiation in the Sichuan basin as well as large areas of the middle and lower reaches of the valley, reaching $R > 0.8$, where the croplands consist of a large portion of paddy fields.

In general, total ET, transpiration, canopy interception, and bare-soil evaporation are mainly controlled by precipitation in the source areas. While in most other areas, solar radiation plays the leading role in total ET, transpiration, bare-soil evaporation, and open-water evaporation. As for canopy interception, it is controlled by precipitation to a high degree throughout the valley and affected by solar radiation to some extent.

The spatial distributions of the partial correlation coefficients of the three constraints applying to total ET and ET components were mapped. As confirmed by Fig. 11a, solar radiation is the dominant factor in deriving ET for the whole basin. There are slight differences in specific areas. In the source region, bare-soil evaporation is the most important component, which is mainly affected by precipitation, so the importance of precipitation to total ET has been emphasized.

Fig. 9 The pixel-wise correlation coefficients between (a1–c1) total ET, (a2–c2) transpiration, (a3–c3) canopy interception, (a4–c4) bare-soil evaporation, and (a5–c5) open-water evaporation with air temperature, precipitation, and solar radiation in the Yangtze River valley for 1980–2014. The shaded areas have passed the 5% significance test



In other regions, vegetation transpiration is far more important than other components. Specifically, in the lower reaches of the Yangtze River and Sichuan basin, vegetation transpiration is mainly affected by both solar radiation and air temperature; thus, solar radiation and air temperature are the two leading factors of total ET. Vegetation transpiration is completely

affected by air temperature in the southwest of the basin where the leading factor of total ET is air temperature. However, in the southeast of the basin, vegetation transpiration is mainly affected by solar radiation, while intercepting loss and bare-soil evaporation which are affected by precipitation jointly make significant contributions to total ET in this region. Therefore, solar radiation and precipitation are the two dominant factors of total ET in this region.

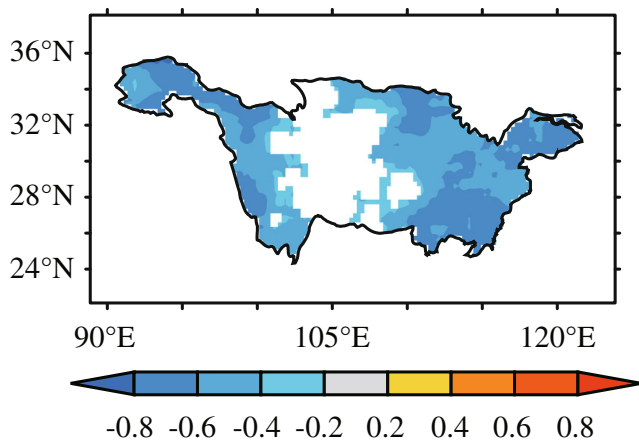
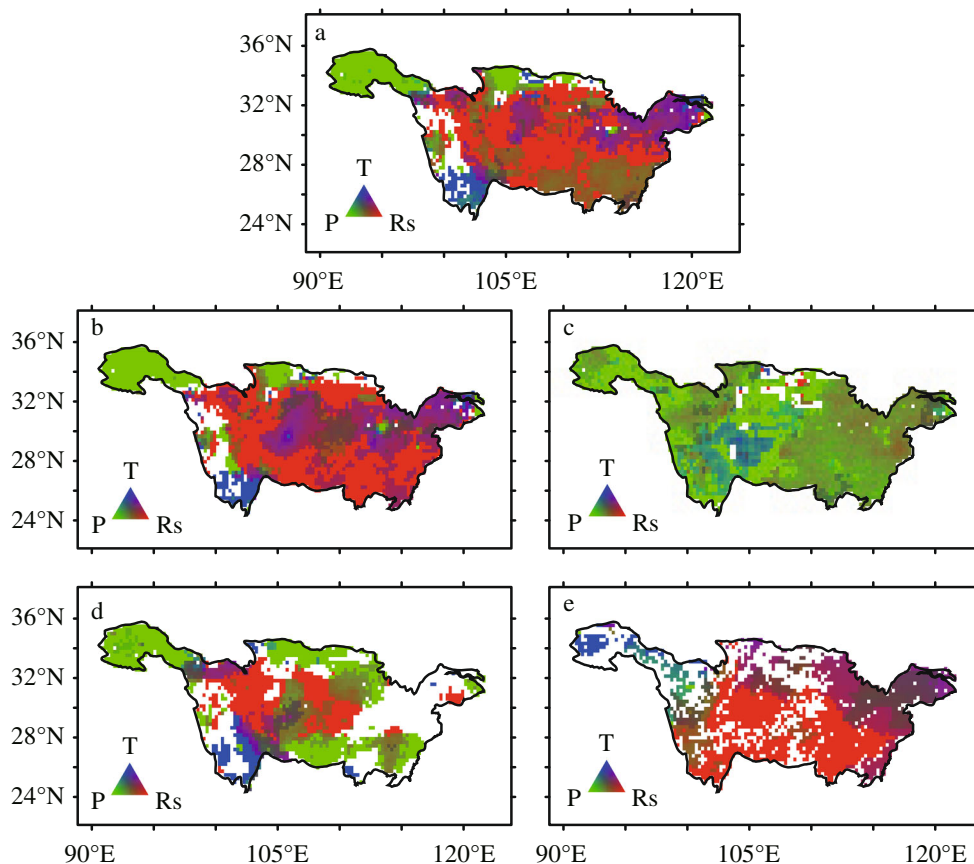


Fig. 10 The pixel-wise correlation coefficients between precipitation and solar radiation. The shaded areas have passed the 5% significance test

Except for air temperature, precipitation, and solar radiation, there are many other factors influencing total ET. Since transpiration plays the dominant role in total ET, we have briefly analyzed the relationship between total ET and NDVI. Figure 12 a shows the variations of NDVI during 1982–2014 in the Yangtze River valley, revealing a significant increasing trend in most areas of the valley, with the speed of 0.01–0.03 per decade. Figure 12 b shows the correlation coefficients between NDVI and total ET, demonstrating significant positive correlations, with the correlation coefficients between 0.4 and 0.8. It means that the variations between NDVI and total ET are consistent, that is, when total ET is not affected by other factors, it increases with vegetation increasing. It can be inferred that vegetation plays a completely positive role

Fig. 11 Spatial distribution of three constraints of air temperature (T), precipitation (P), and surface net solar radiation (Rs) on **a** total ET, **b** transpiration, **c** canopy interception, **d** bare-soil evaporation, and **e** open-water evaporation. Each color corresponds to a unique combination of the partial correlations of the three constraints on ET and its components



throughout the process of total ET. Among the ET components, transpiration is closely related to vegetation. The variations of transpiration and vegetation must be consistent, while other components have little to do with it.

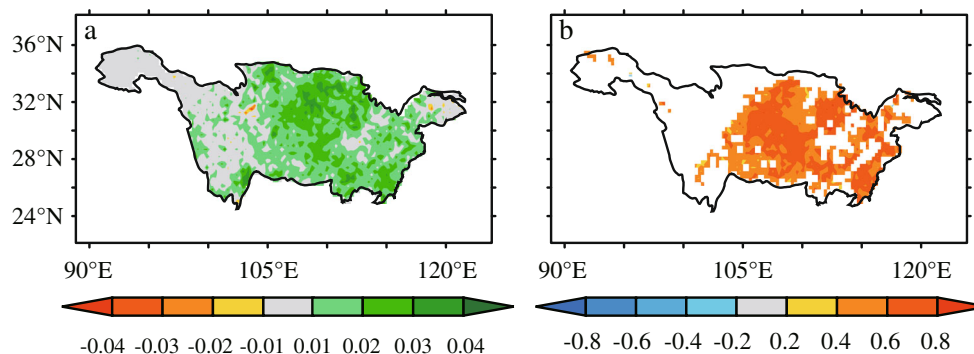
4 Discussions and conclusions

Understanding historical changes in ET would enable a better quantification of the future availability of water across the continents, which in turn, may help to better manage water resources via irrigation scheduling, drought detection, assessment, and so forth. However, evapotranspiration is among the most difficult components of land hydrology to quantify

accurately (Dolman and Jeu 2010). A large number of environmental (e.g., soil moisture, plant phenology, soil properties) and climatic factors (e.g., solar radiation, temperature, humidity, wind speed) can affect the processes of land ET, leading to considerable uncertainties in the ET estimations (Monteith 1965).

As a consequence of the uncertainties of ET estimations, there are debates on the trends of land ET in the past decades in the Yangtze River valley. Gao et al. (2007) estimated the land ET in China for 1960–2002, based on the modified water balance method and meteorological observations, suggesting significant decreasing trends of annual ET in the Yangtze River valley, due to actual evapotranspiration equaling the potential evapotranspiration under wet conditions. Wang

Fig. 12 **a** The spatial distributions of linear trends of NDVI in the Yangtze River valley for the period 1980–2014. The unit is /10a. **b** The pixel-wise correlation coefficients between total ET and NDVI. The shaded areas have passed the 5% significance test



et al. (2011) used the advection-aridity model to estimate land ET from 1961 to 2007 and suggested that the annual ET was significantly decreasing for the decreasing net radiation in the Yangtze River Basin during the period 1961–2007. Using a remote sensing–based ET data of 1982–2013, Zhang et al. (2015a) investigated multidecadal changes in global ET, finding that the annual ET appeared to have significant increasing trend in the Eastern China, mainly driven by vegetation greening, especially in the middle and lower reaches of the Yangtze River basin. Liu et al. (2016) used a process-based ecosystem model to estimate the land ET in China from 2000 to 2014, finding also increasing trend in annual ET in the Yangtze River valley due to vegetation greening. Li et al. (2014) used the revised Remote Sensing–Penman Monteith (RS-PM) model to estimate land ET over China, and increasing trends of annual ET are also found in the Yangtze River valley, which is primarily controlled by variations in incident net radiation. There are also a number of other studies for improving the estimations of land ET, especially from satellite data sources (e.g., Yao et al. 2017; Chen et al. 2015).

Although there are considerable uncertainties in the ET estimations, Chen et al. (2014) have evaluated eight [satellite-based evapotranspiration models using ET data from 23 eddy covariance towers in China](#) and suggested that process-based models generally have better performances than empirical models; this promotes the need for examining the ET component estimations in further studies. Nevertheless, up to date, there are few studies for understanding the contributions of different ET components and their changes in China.

In this study, we have used the state-of-the-art process-based GLEAM ET product which has been evaluated in the Yangtze River valley on the observations of flux and the water balance method to study the changes of land ET and its components during the period 1980–2014. There are added values for this study. First, previous studies in the Yangtze River valley mostly focus on the changes of annual ET, and we have further analyzed the ET changes in different seasons. Second, the ET components are particularly analyzed so as to understand their relative importance in the total land ET and their trends in the recent warming climate.

Our study has indicated a significant increasing trend of annual ET during 1980–2014 in the Yangtze River valley, especially in the middle and lower reaches; this is in agreement with the studies using process-based models which in cooperates satellite data sources, e.g., Li et al. (2014) and Zhang et al. (2015a), Liu et al. (2016). Not surprisingly, it is determined that vegetation transpiration is a dominant ET component in the Yangtze River valley, in line with suggestions from Jasechko et al. (2013) and Schlesinger and Jasechko (2014). The dominance of transpiration has indicated that the biological fluxes are of priority to improve for development of hydrological models in the Yangtze River

valley. It is also found that the increasing trend of land ET is mostly due to the increase of transpiration, indicating vigorous growth of vegetation and increase of food production, which has further demonstrated the critical role of biological processes in the enhanced water cycle in response to climate change.

In the big picture of warming climate, temperature, precipitation, and solar radiation have changed, which may have complex influences on the changes in the land ET over China directly or indirectly. Yang et al. (2016) analyzed the climate change impact on land ET in the Taohe River basin of China, where it features a dry climate, and found precipitation was the most important positive controller of ET changes during 1981–2010. Zhang et al. (2015b) found that precipitation plays a significant positive role in determining the grassland ET in Inner Mongolia, China. Mao and Wang (2017) found that solar radiation plays an important role in deriving ET except arid regions using modified Penman-Monteith model with station-based observational input data. In our analysis of the Yangtze River valley, the spatial pattern of total ET is jointly determined by precipitation and temperature. As for the temporal dynamics, solar radiation is found to be the prevailing factor that controls the interannual variations of total ET.

There are many limiting factors that affect the changes of land ET in the Yangtze River valley. Compared with the total ET analysis, our study of the ET components has made a further step forward for understanding the underlying dynamics of ET changes in the recent decades. Despite this fact, there remains limited understanding of the driving factors for these changes. For example, the transpiration increase cannot be simply attributed to the vegetation increase, although the vegetation has indeed largely increased in the Yangtze River valley. Water supply for vegetation, which is precipitation and consequently soil water content, is the primary limiting factor of transpiration, and furthermore, the increasing stress of atmospheric demand in the warming climate is acting more actively in enhancing land surface fluxes, as Sun et al. (2017) suggested. Hence, more detailed studies, with emphasis on the changing mechanisms of ET components, need to be further conducted.

Author contributions Jiao Lu and Guojie Wang conceived this study and performed the data analysis and wrote the manuscript. All the other authors are actively involved in the discussions.

Funding information This study is supported by National Key Research and Development Program of China (2017YFA0603701) and National Natural Science Foundation of China (41561124014, 41375099).

Compliance with ethical standards

Conflict of interest The authors declare that they have no conflict of interest.

References

- Ali S, Elham F, Mohammad M, Hassan A, Forood S (2013) Estimation of small rainfall events impact on the urban runoff by analytical model. *Eur Res* 42:418–423
- Bai P, Liu X (2018) Intercomparison and evaluation of three global high-resolution evapotranspiration products across China. *J Hydrol* 566: 743–755
- Beck HE, AIJMVan D, Levizzani V, Schellekens J, Miralles DG, Martens B, ADe R (2017) MSWEP: 3-hourly 0.25° global gridded precipitation (1979–2015) by merging gauge satellite and reanalysis data. *Hydrol Earth Syst Sci* 21:1–38
- Chen Y, Xia J, Liang S, Feng J, Fisher JB, Li X, Li X (2014) Comparison of satellite-based evapotranspiration models over terrestrial ecosystems in China. *Remote Sens Environ* 140:279–293
- Chen Y, Yuan W, Xia J, Fisher JB, Dong W, Zhang X, Liang S, Ye A, Cai W, Feng J (2015) Using Bayesian model averaging to estimate terrestrial evapotranspiration in China. *J Hydrol* 528:537–549
- Dolman AJ, Jeu RAMD (2010) Evaporation in focus. *Nat Geosci* 3:296
- Dooge J (1975) The water balance of bogs and fens. Review report Stud Reports Hydrol 19
- Douville H, Ribes A, Decharme B, Alkama R, Sheffield J (2012) Anthropogenic influence on multidecadal changes in reconstructed global evapotranspiration. *Nat Clim Chang* 3:59–62
- Fisher JB, Melton F, Middleton E, Hain C, Anderson M, Allen R, McCabe M, Hook S, Baldocchi D, Townsend PA, Kilic A, Tu K, Miralles DD, Perret J, Lagouarde J, Waliser D, Purdy AJ, French A, Schimel D, Famiglietti JS, Stephens G, Wood EF (2017) The future of evapotranspiration: global requirements for ecosystem functioning, carbon and climate feedbacks, agricultural management, and water resources. *Water Resour Res* 53:2618–2626
- Fu BP (1981) On the calculation of the evaporation from land surface. *Sci Atmos Sin* 5:23–31 in Chinese
- Gao G, Chen D, Xu C, Simelton E (2007) Trend of estimated actual evapotranspiration over China during 1960–2002. *J Geophys Res* 112:D11120
- Gong D, Kang S, Yao L, Zhang L (2007) Estimation of evapotranspiration and its components from an apple orchard in Northwest China using sap flow and water balance methods. *Hydrol Process* 21:931–938
- Greve P, Orlowsky B, Mueller B, She J, Reichstein M, Seneviratne SI (2014) Global assessment of trends in wetting and drying over land. *Nat Geosci* 7:716–721
- Greve P, Gudmundsson L, Orlowsky B, Seneviratne S (2015) Introducing a probabilistic Budyko framework. *Geophys Res Lett* 42:2261–2269
- Guillod B, Orlowsky B, Miralles DG, Teuling AJ, Seneviratne SI (2015) Reconciling spatial and temporal soil moisture effects on afternoon rainfall. *Nat Commun* 6:6443
- Jasechko S, Sharp ZD, Gibson JJ, Birks SJ, Yi Y, Fawcett PJ (2013) Terrestrial water fluxes dominated by transpiration. *Nature* 496: 347–350
- Jime C, Prigent C, Aires F (2009) Toward an estimation of global land surface heat fluxes from multisatellite observations. *J Geophys Res* 114:D06305
- Jung M, Reichstein M, Bondeau A (2009) Towards global empirical upscaling of FLUXNET eddy covariance observations: validation of a model tree ensemble approach using a biosphere model. *Biogeosci Discuss* 6:5271–5304
- Jung M, Reichstein M, Ciais P, Seneviratne SI, Sheffield J, Goulden ML, Bonan G, Cescatti A, Chen J, RDe J, Dolman AJ, Eugster W, Gerten D, Gianelle D, Gobron N, Heinke J, Kimball J, Law BE, Montagnani L, Mu Q, Mueller B (2010) Recent decline in the global land evapotranspiration trend due to limited moisture supply. *Nature* 467:951–954
- Li X, Liang S, Yuan W, Yu G, Cheng X, Chen Y, Zhao T, Feng J, Ma Z, Ma M, Liu S, Chen J (2014) Estimation of evapotranspiration over the terrestrial ecosystems in China. *Ecohydrology* 7:139–149
- Lin Y, Wang GX, Guo JY, Sun XY (2012) Quantifying evapotranspiration and its components in a coniferous subalpine forest in Southwest China. *Hydrol Process* 26:3032–3040
- Liou Y, Kar SK (2014) Evapotranspiration estimation with remote sensing and various surface energy balance algorithms—a review. *Energies* 7:2821–2849
- Liu Y, Xiao J, Ju W, Xu K, Zhou Y, Zhao Y (2016) Recent trends in vegetation greenness in China significantly altered annual evapotranspiration and water yield. *Environ Res Lett* 11:94010
- Lockwood JG (1990) The influence of temperature variations on interception loss and water storage in vegetation canopies. *Water Resour Res* 26:941–943
- Lv J, Ren J, Ju J (2004) The interdecadal variability of East Asia monsoon and its effect on the rainfall over China. *J Trop Meteorol* 20:73–80
- Mao Y, Wang K (2017) Comparison of evapotranspiration estimates based on the surface water balance, modified Penman-Monteith model, and reanalysis data sets for continental China. *J Geophys Res-Atmos* 122:3228–3244
- Mao Y, Wang K, Liu X, Liu C (2016) Water storage in reservoirs built from 1997 to 2014 significantly altered the calculated evapotranspiration trends over China. *J Geophys Res-Atmos* 121:10,097–010, 112
- Miralles DG, Holmes TRH, RAMDe J, Gash JH, Meesters AGCA, Dolman AJ (2011a) Global land-surface evaporation estimated from satellite-based observations. *Hydrol Earth Syst Sci* 15:453–469
- Miralles DG, RAMDe J, Gash JH, Holmes TRH, Dolman AJ (2011b) Magnitude and variability of land evaporation and its components at the global scale. *Hydrol Earth Syst Sci Discuss* 15:967–981
- Miralles DG, MJVanDen B, Gash JH, Parinussa RM (2014a) El Niño–La Niña cycle and recent trends in continental evaporation. *Nat Clim Chang* 4:122–126
- Miralles DG, Teuling AJ, CCVan H (2014b) Mega-heatwave temperatures due to combined soil desiccation and atmospheric heat accumulation. *Nat Geosci* 7:345–349
- Mo X, Liu S, Lin Z, Wang S, Hu S, Liu S, Lin Z, Wang S, Trends SH (2015) Trends in land surface evapotranspiration across China with remotely sensed NDVI and climatological data for 1981–2010. *Hydrol Sci J* 60:2163–2177
- Modares R, Paulo VD (2007) Rainfall trends in arid and semi-arid regions of Iran. *J Arid Environ* 70:344–355
- Monteith JL (1965) Evaporation and environment. *Symp Soc Exp Biol* 19:205–234
- Mu Q, Zhao M, Running SW (2011) Improvements to a MODIS global terrestrial evapotranspiration algorithm. *Remote Sens Environ* 115: 1781–1800
- Mueller B, Hirschi M, Jimenez C, Ciais P, Dirmeyer PA, Dolman AJ (2013) Benchmark products for land evapotranspiration: LandFlux-EVAL multi-dataset synthesis. *Hydrol Earth Syst Sci Discuss* 10:769–805
- Oki T, Kanae S (2006) Global hydrological cycles and world water resources. *Science* 313:1068–1072
- Peng J, Li Y, Tian L, Liu Y, Wang Y (2015) Vegetation dynamics and associated driving forces in eastern China during 1999–2008. *Remote Sens* 7:13641–13663
- Pinzon J, Tucker C (2014) A non-stationary 1981–2012 AVHRR NDVI3G time series. *Remote Sens* 6:6929–6960
- Priestley CHB, Taylor RJ (1972) On the assessment of surface heat flux and evaporation using large-scale parameters. *Mon Weather Rev* 100:81–92
- Ribeiro L, Kretschmer N, Nascimento J, Buxo A, Rötting T, Soto G, Señoret M (2015) Evaluating piezometric trends using the Mann-Kendall test on the alluvial aquifers of the Elqui River basin Chile. *Hydrol Sci J* 60:1840–1852

- Schlesinger WH, Jasechko S (2014) Transpiration in the global water cycle. *Agric For Meteorol* 189–190:115–117
- Sen PK (1968) Estimates of the regression coefficient based on Kendall's tau. *J Am Stat Assoc* 63:1379–1389
- Senay GB, Leake S, Nagler PL, Artan G, Dickinson J, Cordova JT, Glenn EP (2011) Estimating basin scale evapotranspiration (ET) by water balance and remote sensing methods. *Hydrol Process* 25:4037–4049
- Shi Z, Shan N, Xu L, Yang X, Gao J, Guo H, Zhang X (2016) Spatiotemporal variation of temperature precipitation and wind trends in a desertification prone region of China from 1960 to 2013. *Int J Climatol* 36:4327–4337
- Simmons A, Uppala SM, Dee D, Kobayashi S (2007) ERA-Interim: new ECMWF reanalysis products from 1989 onwards. *ECMWF Newsl* 110:25–35
- Su B, Jiang T, Shi Y, Becker S, GEMMER M (2004) Observed precipitation trends in the Yangtze river catchment from 1951 to 2002. *J Geogr Sci* 14:204–218
- Sun S, Chen H, Ju W, Yu M, Hua W, Yin Y (2014) On the attribution of the changing hydrological cycle in Poyang Lake. *J Hydrol* 514:214–225
- Sun S, Chen H, Ju W, Wang G, Sun G (2017) On the coupling between precipitation and potential evapotranspiration: contributions to decadal drought anomalies in the Southwest China. *Clim Dyn* 48:3779–3797
- Taylor CM, RAMde J, Guichard F, Harris PP, Dorigo WA (2012) Afternoon rain more likely over drier soils. *Nature* 489:423–426
- Theil H (1950) A rank-invariant method of linear and polynomial regression analysis I II III. *Nederl akad wetensch proc* 12:345–381
- Tian Q, Yang S (2017) Regional climatic response to global warming: trends in temperature and precipitation in the Yellow Yangtze and Pearl River basins since the 1950s. *Quat Int* 440:1–11
- Wang K, Dickinson RE (2012) A review of global terrestrial evapotranspiration: observation modeling climatology and climatic variability. *Rev Geophys* 50:RG2005
- Wang X, Zhou Y (2016) Shift of annual water balance in the Budyko space for catchments with groundwater-dependent evapotranspiration. *Hydrol Earth Syst Sc* 20:3673–3690
- Wang K, Dickinson RE, Wild M, Liang S (2010a) Evidence for decadal variation in global terrestrial evapotranspiration between 1982 and 2002: 1. Model development. *J Geophys Res* 115:D20112
- Wang K, Dickinson RE, Wild M, Liang S (2010b) Evidence for decadal variation in global terrestrial evapotranspiration between 1982 and 2002: 2. Results. *J Geophys Res* 115:D20113
- Wang Y, Liu B, Su B, Zhai J, GEMMER M (2011) Trends of calculated and simulated actual evaporation in the Yangtze River basin. *J Clim* 24:4494–4507
- Xu T, Guo Z, Liu S, He X, Meng Y, Xu Z, Xia Y, Xiao J, Zhang Y, Ma Y, Song L (2018) Evaluating different machine learning methods for upscaling evapotranspiration from flux towers to the regional scale. *J Geophys Res-Atmos* 123:8674–8690
- Yang X, Wang G, Ye J (2015) Spatial and temporal changing analysis of terrestrial evapotranspiration in Huai River basin based on GLEAM data. *Trans Chinese Soc Agric Eng* 31:133–139
- Yang L, Feng Q, Li C, Si J, Wen X, Yin Z (2016) Detecting climate variability impacts on reference and actual evapotranspiration in the Taohe River basin NW China. *Hydrol Res* 48:596–612
- Yang X, Yong B, Ren L, Zhang Y, Long D (2017) Multi-scale validation of GLEAM evapotranspiration products over China via China FLUX ET measurements. *Int J Remote Sens* 38:5688–5709
- Yao Y, Liang S, Qin Q, Wang K, Liu S, Zhao S (2012) Satellite detection of increases in global land surface evapotranspiration during 1984–2007. *Int J Digit Earth* 5:299–318
- Yao Y, Liang S, Li X, Chen J, Liu S, Jia K, Zhang X, Xiao Z, Fisher JB, Mu Q, Pan M, Liu M, Cheng J, Jiang B, Xie X, Grünwald T, Bernhofer C, Roupsard O (2017) Improving global terrestrial evapotranspiration estimation using support vector machine by integrating three process-based algorithms. *Agric For Meteorol* 242:55–74
- Zamani R, Mirabbasi R, Abdollahi S, Shajharia D (2017) Streamflow trend analysis by considering autocorrelation structure long-term persistence and Hurst coefficient in a semi-arid region of Iran. *Theor Appl Climatol* 129:33–45
- Zhang L, Potter N, Hickel K, Zhang Y, Shao Q (2008) Water balance modeling over variable time scales based on the Budyko framework – model development and testing. *J Hydrol* 360:117–131
- Zhang S, Yu P, Wang Y, Zhang H, Krysanova V, Huang S, Xiong W, Xu L (2011) Estimation of actual evapotranspiration and its component in the upstream of Jinghe basin. *Acta Geograph Sin* 66:385–395
- Zhang K, Kimball JS, Nemani RR, Running SW, Hong Y, Gourley JJ, Yu Z (2015a) Vegetation greening and climate change promote multidecadal rises of global land evapotranspiration. *Sci Rep* 5:15956
- Zhang S, Shen R, Zhao H, Liu T, Shao H, Zhang Z (2015b) Correlating between evapotranspiration and precipitation provides insights into Xilingol grassland eco-engineering at larger scale. *Ecol Eng* 84:100–103
- Zhang Y, Kong D, Gan R, Chiew FHS, McVicar TR, Zhang Q, Yang Y (2019) Coupled estimation of 500 m and 8-day resolution global evapotranspiration and gross primary production in 2002–2017. *Remote Sens Environ* 222:165–182
- Zhou Z, Wang H, Zhong B, Luo Z, Li Q (2016) Evapotranspiration estimation over Yangtze River basin from GRACE satellite measurement and in situ data. *Egu General Assembly Conference* 18

Publisher's note Springer Nature remains neutral with regard to jurisdictional claims in published maps and institutional affiliations.